

# Symmetric quantum joint measurements on multiple qubits

Dong Ding<sup>1</sup>, Ying-Qiu He<sup>1,\*</sup>, Ting Gao<sup>2,†</sup> and Feng-Li Yan<sup>3‡</sup>

<sup>1</sup> College of Science, North China Institute of Science and Technology, Beijing 101601, China

<sup>2</sup> School of Mathematical Sciences, Hebei Normal University, Shijiazhuang 050024, China

<sup>3</sup> College of Physics, Hebei Key Laboratory of Photophysics Research and Application, Hebei Normal University, Shijiazhuang 050024, China

(Dated: March 13, 2025)

We investigate the generalization of symmetric quantum joint measurements on multiple qubits. We first describe a method for constructing a symmetric joint measurement basis for three qubits by utilizing single-qubit states corresponding to the four vertices of a tetrahedron on the Bloch sphere. We demonstrate the expected tetrahedral symmetry of the current measurement basis and discuss its application in a triloca star-shaped network. This architecture enables us to generalize the two-qubit symmetric joint measurement to an  $n$ -qubit version, preserving the tetrahedral or hexahedral symmetry.

PACS numbers: 03.65.Ud; 03.67.-a; 03.67.Mn

## I. INTRODUCTION

Quantum measurement is a cornerstone of quantum mechanics and underlies the concepts of quantum computation and quantum information processing [1, 2]. It includes both single-system measurements and composite-system joint measurements. The well-known Bell state measurement (BSM) and its generalized forms serve as the canonical method for detecting multi-qubit systems [3].

In 2019, a novel symmetric joint measurement for two qubits, termed the *elegant joint measurement* (EJM), was proposed by Gisin [4]. The symmetry of the EJM basis is mainly reflected in that both the single-qubit ingredient and the reduced states are precisely associated with the four vertices of a specified tetrahedron. After Gisin's idea, Tavakoli *et al.* [5] proposed the parameterized EJM by introducing a real parameter  $\theta \in [0, \pi/2]$ . This formulation retains the elegant symmetry, allowing it to encompass both the EJM and the conventional BSM. The EJM basis states were initially designed for testing non-bilocal correlations [6–11] and it has been experimentally confirmed via superconducting quantum processors [12] as well as hyperentangled photons [13]. Recently, Del Santo *et al.* [14] have proposed an in-depth study on two-qubit entangled measurements. In their work, the authors offered a complete classification of two-qubit bases that have the same degree of entanglement. They also suggested that an iso-entangled basis for two qubits typically depends on three parameters. In view of this, He *et al.* [15] extended the single-parameter EJM to three-parameter EJM. It offers a broader range of points on the Bloch sphere (unit vectors) that are suitable for constructing the generalized EJM basis. However, compared to the generalized BSM (or GHZ-state measurement), it does not appear to be an issue that can be naturally generalized, due to the constraints imposed by tetrahedral symmetry.

In the present paper, we focus on multi-qubit symmetric joint measurements. We first define a three-qubit EJM basis by using the three-parameter EJM and verify their tetrahedral symmetry. Next, we apply the three-qubit EJM to the triloca star-shaped network, effectively demonstrating network nonlocality. Finally, we provide a method to develop the multi-qubit EJM bases and analyze its symmetry.

## II. SYMMETRIC JOINT MEASUREMENTS ON TWO QUBITS

We here review two-qubit symmetric joint measurements. Consider four pure single-qubit states

$$|m_i\rangle = \frac{1}{\sqrt{2}}(\sqrt{1+z_i}e^{-i\varphi_i/2}|0\rangle + \sqrt{1-z_i}e^{i\varphi_i/2}|1\rangle), \quad i = 0, 1, 2, 3, \quad (1)$$

---

\*Electronic address: heyq@ncist.edu.cn

†Electronic address: gaoting@hebtu.edu.cn

‡Electronic address: flyan@hebtu.edu.cn

each of which is respectively associated with a unit vector

$$\vec{m}_i = \langle m_i | \vec{\sigma} | m_i \rangle = (\sqrt{1-z_i^2} \cos \varphi_i, \sqrt{1-z_i^2} \sin \varphi_i, z_i). \quad (2)$$

Here,  $\vec{\sigma} = (\sigma_x, \sigma_y, \sigma_z)$  is the vector of Pauli matrices, the real parameters  $|z_i| \leq 1$  and  $\varphi_i \in [-\pi, \pi]$ .

Choosing  $\varphi_0 = \pi/4$ ,  $\varphi_1 = -\pi/4$ ,  $\varphi_2 = 3\pi/4$ ,  $\varphi_3 = -3\pi/4$ ,  $z_0 = z_3 = 1/\sqrt{3}$ ,  $z_1 = z_2 = -1/\sqrt{3}$ , i.e.,

$$\vec{m}_0 = (1, 1, 1)/\sqrt{3}, \quad \vec{m}_1 = (1, -1, -1)/\sqrt{3}, \quad \vec{m}_2 = (-1, 1, -1)/\sqrt{3}, \quad \vec{m}_3 = (-1, -1, 1)/\sqrt{3}, \quad (3)$$

one can define a set of two-qubit basis, parameter-free EJM [4], as

$$|\Phi_i\rangle = \frac{1}{2\sqrt{2}}[(\sqrt{3}+1)|m_i, -m_i\rangle + (\sqrt{3}-1)|-m_i, m_i\rangle], \quad i = 0, 1, 2, 3, \quad (4)$$

where  $|-m_i\rangle = (1/\sqrt{2})(\sqrt{1-z_i}e^{-i\varphi_i/2}|0\rangle - \sqrt{1+z_i}e^{i\varphi_i/2}|1\rangle)$  is orthogonal to  $|m_i\rangle$ .

It can be further parameterized by incorporating a variable  $\theta \in [0, \pi/2]$ , single-parameter EJM [5], as

$$|\Phi_i^\theta\rangle = \frac{1}{2\sqrt{2}}[(\sqrt{3}+e^{i\theta})|m_i, -m_i\rangle + (\sqrt{3}-e^{i\theta})|-m_i, m_i\rangle], \quad (5)$$

such that it seamlessly interpolates between the EJM ( $\theta = 0$ ) and the normal BSM ( $\theta = \pi/2$ ).

Note that a two-qubit symmetric joint measurement is generally characterized by three parameters [14]. Consider three real parameters  $1/\sqrt{3} \leq |z| \leq 1$ ,  $\varphi \in [-\pi, \pi]$  and  $\theta \in [0, \pi/2]$ . A more generalized symmetric joint measurement, three-parameter EJM [15], is then given by

$$|\Phi_0(z, \varphi, \theta)\rangle = \frac{1-i\sqrt{3z^2-1}}{2\sqrt{3z^2}}[e^{-i(\varphi-\varphi_z)}|00\rangle - r_+^\theta|01\rangle - r_-^\theta|10\rangle - e^{i(\varphi-\varphi_z)}|11\rangle], \quad (6)$$

$$|\Phi_1(z, \varphi, \theta)\rangle = \frac{1-i\sqrt{3z^2-1}}{2\sqrt{3z^2}}[-ie^{-i(\varphi-\varphi_z)}|00\rangle + r_-^\theta|01\rangle + r_+^\theta|10\rangle - ie^{i(\varphi-\varphi_z)}|11\rangle], \quad (7)$$

$$|\Phi_2(z, \varphi, \theta)\rangle = \frac{1-i\sqrt{3z^2-1}}{2\sqrt{3z^2}}[-e^{-i(\varphi-\varphi_z)}|00\rangle - r_+^\theta|01\rangle - r_-^\theta|10\rangle + e^{i(\varphi-\varphi_z)}|11\rangle], \quad (8)$$

$$|\Phi_3(z, \varphi, \theta)\rangle = \frac{1-i\sqrt{3z^2-1}}{2\sqrt{3z^2}}[ie^{-i(\varphi-\varphi_z)}|00\rangle + r_-^\theta|01\rangle + r_+^\theta|10\rangle + ie^{i(\varphi-\varphi_z)}|11\rangle], \quad (9)$$

where  $\varphi_z = \arg[(\sqrt{1-z^2} + i\sqrt{3z^2-1})/(\sqrt{2}|z|)]$  and  $r_\pm^\theta = (1 \pm e^{i\theta})/\sqrt{2}$ . It is not difficult to see that, if one takes  $\varphi - \varphi_z = \pi/4$ , then the three-parameter EJM can naturally be reduced to single-parameter EJM.

From the perspective of quantifying entanglement, all the EJM basis states have the same degree of entanglement. Furthermore, by computing the partial traces one can observe that these EJM bases have elegant symmetry properties: (i) The single-qubit reductions, obtained by tracing out one of the qubits, are mirror images of each other; and (ii) the four points, to which the reduced states of the EJM basis point, form a tetrahedron inside the Bloch sphere.

### III. SYMMETRIC JOINT MEASUREMENTS ON THREE QUBITS

#### A. Definition of three-qubit measurement basis

Consider four real parameters  $1/\sqrt{3} \leq |z| \leq 1$ ,  $\varphi \in [-\pi, \pi]$ ,  $\theta \in [0, \pi/2]$ , and  $\gamma \in [0, \pi/2]$ , and let  $\varphi_0 = \varphi$ ,  $\varphi_1 = \varphi + \pi/2$ ,  $\varphi_2 = \varphi + \pi$ ,  $\varphi_3 = \varphi - \pi/2$ ,  $z_0 = z_2 = z$ ,  $z_1 = z_3 = -z$ . Define eight three-qubit pure states

$$|\Psi_i^0\rangle = \cos \gamma |\Phi_i\rangle |m_i\rangle + (-1)^{\lfloor \frac{i}{2} \rfloor} \sin \gamma |\Phi'_i\rangle |-m_i\rangle, \quad i = 0, 1, 2, 3 \quad (10)$$

and

$$|\Psi_i^1\rangle = \cos \gamma |\Phi_i\rangle |-m_i\rangle - (-1)^{\lfloor \frac{i}{2} \rfloor} \sin \gamma |\Phi'_i\rangle |m_i\rangle, \quad i = 0, 1, 2, 3, \quad (11)$$

where

$$|\Phi_i\rangle = \frac{1 - i\sqrt{3z^2 - 1}}{2\sqrt{3z^2}} [e^{-i(\varphi_i - \varphi_z)}|00\rangle - \frac{1}{\sqrt{2}}[(-1)^i + e^{i\theta}]|01\rangle - \frac{1}{\sqrt{2}}[(-1)^i - e^{i\theta}]|10\rangle - e^{i(\varphi_i - \varphi_z)}|11\rangle] \quad (12)$$

and

$$|\Phi'_i\rangle = \frac{1 - i\sqrt{3z^2 - 1}}{2\sqrt{3z^2}} [-e^{-i(\varphi_i - \varphi_z)}|00\rangle - \frac{1}{\sqrt{2}}[(-1)^i + e^{i\theta}]|01\rangle - \frac{1}{\sqrt{2}}[(-1)^i - e^{i\theta}]|10\rangle + e^{i(\varphi_i - \varphi_z)}|11\rangle] \quad (13)$$

are all the three-parameter two-qubit EJM basis states satisfying  $\langle\Phi_i|\Phi_j\rangle = \delta_{ij}$  and  $\langle\Phi'_i|\Phi'_j\rangle = \delta_{ij}$ ,  $i, j = 0, 1, 2, 3$ ,  $\varphi_z = \arg[(\sqrt{1 - z^2} + i\sqrt{3z^2 - 1})/(\sqrt{2}|z|)]$ ,  $|\pm m_i\rangle = (\sqrt{1 \pm z_i}e^{-i\varphi_i/2}|0\rangle \pm \sqrt{1 \mp z_i}e^{i\varphi_i/2}|1\rangle)/\sqrt{2}$  are single-qubit basis states, as described earlier. Here, the floor function  $[\frac{i}{2}] = 0$  for  $i = 0, 1$ , and  $[\frac{i}{2}] = 1$  for  $i = 2, 3$ . Then,  $\{|\Psi_i^k\rangle\}$  form a three-qubit EJM basis, where  $i = 0, 1, 2, 3$ , and  $k = 0, 1$ .

The proof of the orthogonality and completeness is provided in Appendix A. We next see the tetrahedral symmetry of the present three-qubit basis states.

### B. Entanglement measure and tetrahedral symmetry

An important three-qubit measure of entanglement for pure states is the three-tangle introduced in Ref. [16]. We calculate the three-tangle of the state  $|\Psi_i^k\rangle$  by

$$\tau(|\Psi_i^k\rangle) = 4|(a_{000}a_{111} - a_{001}a_{110})^2 + (a_{010}a_{101} - a_{100}a_{011})^2 + 4(a_{000}a_{110}a_{101}a_{011} + a_{111}a_{001}a_{010}a_{100}) - 2(a_{000}a_{111} + a_{001}a_{110})(a_{010}a_{101} + a_{100}a_{011})|, \quad (14)$$

where the coefficients  $a_{j_1 j_2 j_3} = \langle j_1 j_2 j_3 | \Psi_i^k \rangle$ ,  $j_1, j_2, j_3 = 0, 1$ . A straightforward calculation shows that

$$\tau(|\Psi_i^k\rangle) = \sin^2(2\gamma) \sin \theta, \quad i = 0, 1, 2, 3, \quad k = 0, 1. \quad (15)$$

Based on this observation, the current EJM basis is a three-qubit iso-entangled basis [17]. These basis states exhibit the same degree of entanglement parameterized by  $\gamma$  and  $\theta$ , ranging continuously from 0 to 1. Typically, if one takes  $\gamma = \pi/4$  and  $\theta = \pi/2$ , then it provides the maximally entangled measurement with  $\tau = 1$ ; while for  $\gamma = 0$  (or  $\pi/2$ ) or  $\theta = 0$ , we have  $\tau = 0$  corresponding to the product states.

We now reveal its inherent symmetry by calculating the partial traces (single-qubit reductions of these basis states). By using the results  $\langle m_i | \vec{\sigma} | m_i \rangle = -\langle -m_i | \vec{\sigma} | -m_i \rangle = \vec{m}_i$  and  $\langle \Phi_i | \vec{\sigma} \otimes I | \Phi_i \rangle = -\langle \Phi_i | I \otimes \vec{\sigma} | \Phi_i \rangle = (\cos \theta / \sqrt{2})(\cos(\varphi_i - \varphi_z), \sin(\varphi_i - \varphi_z), (-1)^i / \sqrt{2})$ ,  $i = 0, 1, 2, 3$ , we have

$$\langle \Psi_i^k | \vec{\sigma} \otimes I \otimes I | \Psi_i^k \rangle = \frac{1}{2}[\sqrt{1 + 2\cos^2(2\gamma)} \cos \theta] \vec{m}'_i, \quad (16)$$

$$\langle \Psi_i^k | I \otimes \vec{\sigma} \otimes I | \Psi_i^k \rangle = -\frac{1}{2}[\sqrt{1 + 2\cos^2(2\gamma)} \cos \theta] \vec{m}'_i, \quad (17)$$

and

$$\langle \Psi_i^k | I \otimes I \otimes \vec{\sigma} | \Psi_i^k \rangle = (-1)^k \cos(2\gamma) \vec{m}_i, \quad (18)$$

where  $\vec{m}_i$  (see Eq. (2)) and

$$\vec{m}'_i = \frac{1}{\sqrt{1 + 2\cos^2(2\gamma)}} (\sqrt{2} \cos(2\gamma) \cos(\varphi_i - \varphi_z), \sqrt{2} \cos(2\gamma) \sin(\varphi_i - \varphi_z), (-1)^i) \quad (19)$$

are two unit vectors that can respectively configure a tetrahedron on the Bloch sphere. A detailed derivation of the Eqs. (16)–(18) is presented in Appendix B.

The symmetry of the current basis states is reflected in the following two aspects: (i) The reductions of the EJM basis states result in two pairs of mirror-image tetrahedra: one pair, with a radius (circumradius) of  $\cos(2\gamma)$ , has its four vertices aligned with the vectors  $\vec{m}_i$  and  $-\vec{m}_i$ ; the other pair, with a radius of  $(1/2)\sqrt{1 + 2\cos^2(2\gamma)} \cos \theta$ , has

its vertices directed towards the vectors  $\vec{m}'_i$  and  $-\vec{m}'_i$ . (ii) The cumulative sum of all vectors associated with the reduced states amounts to zero, i.e.,

$$\sum_{i,k} (\langle \Psi_i^k | \vec{\sigma} \otimes I \otimes I | \Psi_i^k \rangle + \langle \Psi_i^k | I \otimes \vec{\sigma} \otimes I | \Psi_i^k \rangle + \langle \Psi_i^k | I \otimes I \otimes \vec{\sigma} | \Psi_i^k \rangle) = 0. \quad (20)$$

It is not difficult to see that, the parameters  $\gamma$ ,  $z$ , and  $\varphi$  determine the positions to which the vectors point. To be more specific, if one takes  $\gamma = 0$  and  $z = 1/\sqrt{3}$ , then the unit vectors  $\vec{m}'_i = \vec{m}_i$ , and thus all reductions of the EJM basis states direct towards one of the same mirror-image vectors  $\pm(\sqrt{2} \cos \varphi_i, \sqrt{2} \sin \varphi_i, (-1)^i)/\sqrt{3}$ ; if one takes  $\gamma = \pi/4$ , then a pair of tetrahedra reduces to a point with a radius of zero, and the other pair of tetrahedra reduces to two mirror-image points  $(0, 0, 1)$  and  $(0, 0, -1)$ . While the parameters  $\theta$  and  $\gamma$  affect the modulus of these vectors, in particular, if one takes  $(1/2)\sqrt{1 + 2 \cos^2(2\gamma)} \cos \theta = \cos(2\gamma)$ , then the radii of these tetrahedra are equal. For  $\theta = \pi/2$  and  $\gamma = \pi/4$ , related to the maximally entangled measurement  $\tau = 1$ , all radii of the tetrahedra are zero; for  $\theta = 0$  (thus  $\tau = 0$ ) and  $\gamma = \pi/8$ , then all the tetrahedra have equal radii of  $1/\sqrt{2}$ .

## IV. AN APPLICATION TO A TRILOCAL STAR NETWORK

### A. The star-network configuration and trilocality inequality

In this section, we investigate the star-network nonlocalities using the current EJM basis. Consider a triloal star-shaped network with three extremal parties Alices ( $A_i, i = 1, 2, 3$ ) and a central party Bob ( $B$ ), as shown in Fig.1. Suppose that there are three independent (space-like separated) two-particle sources, each of which sends one particle to  $A_i$  and  $B$ , respectively. Each extremal party  $A_i$  performs a dichotomic measurement with inputs  $x_i$  and outputs  $a_i$  (where  $x_i, a_i = 0, 1$ ), while the central party  $B$  always performs a fixed three-qubit joint measurement and then obtains one of eight possible outputs  $b = b_1 b_2 b_3$  where  $b_1, b_2, b_3 = 0, 1$ .

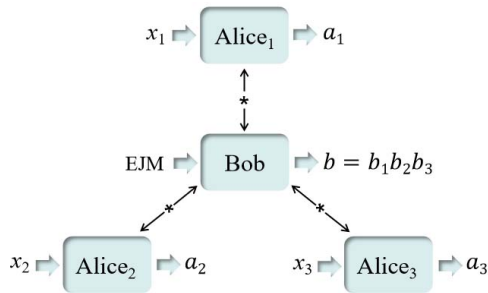


FIG. 1: A triloal star-shaped network with three extremal parties (Alice<sub>1</sub>, Alice<sub>2</sub>, and Alice<sub>3</sub>) performing dichotomic measurements, respectively, and the central party Bob carrying out a fixed three-qubit joint measurement.

In such a case, consider the triloal correlation quantities [7]

$$I_m = \frac{1}{2^3} \sum_{x_1, x_2, x_3} (-1)^{g_m(x_1, x_2, x_3)} \langle A_{x_1}^1 A_{x_2}^2 A_{x_3}^3 B^m \rangle, \quad m = 1, 2, 3, 4, \quad (21)$$

with the correlator

$$\langle A_{x_1}^1 A_{x_2}^2 A_{x_3}^3 B^m \rangle = \sum_{a_1, a_2, a_3, b^1, b^2, b^3, b^4} (-1)^{a_1 + a_2 + a_3 + b^m} P(a_1 a_2 a_3 b^1 b^2 b^3 b^4 | x_1 x_2 x_3), \quad (22)$$

where  $g_1(x_1, x_2, x_3) = 0$ ,  $g_2(x_1, x_2, x_3) = x_1 + x_2$ ,  $g_3(x_1, x_2, x_3) = x_1 + x_3$ ,  $g_4(x_1, x_2, x_3) = x_2 + x_3$ , each  $b^m$  (with  $b^m = 0, 1$ ), corresponding to the operator  $B^m$ , is a processed bit derived from the raw outputs  $b$ , and  $P(a_1 a_2 a_3 b^1 b^2 b^3 b^4 | x_1 x_2 x_3)$  is a probability distribution on the triloal star network.

Then, in the current trilocality configuration, the following inequality

$$\sum_{m=1}^4 |I_m|^{1/3} \leq 2 \quad (23)$$

holds for every triloal probability distributions [7]. If a quantum prediction exceeds the classical constraint, i.e., the inequality is violated by a quantum system, then the star-network exhibits quantum nonlocality.

## B. Quantum violations

Suppose that each quantum source produces two-qubit pure state  $|\Psi^+\rangle = (|01\rangle + |10\rangle)/\sqrt{2}$ . For each of the three extremal parties Alices, choose  $A_0^i = (\sigma_x + \sigma_z)/\sqrt{2}$  or  $A_1^i = (\sigma_x - \sigma_z)/\sqrt{2}$  on their single-qubit subsystem. The central party Bob performs a fixed EJM on her three-qubit subsystem. In detail, let

$$B^m = M_0^m - M_1^m, \quad m = 1, 2, 3, 4, \quad (24)$$

where

$$M_b^m = \sum_{b_1 b_2 b_3} \delta_{b, b^m} |\Psi_{b_1 b_2 b_3}\rangle \langle \Psi_{b_1 b_2 b_3}|, \quad m = 1, 2, 3, 4, \quad b = 0, 1, \quad b_1, b_2, b_3 = 0, 1, \quad (25)$$

and bit  $b^m = b^m(b_1, b_2, b_3)$ . To proceed, we define the bits

$$b^1 = b_2 \oplus b_3 \oplus 1, \quad b^2 = b_3, \quad b^3 = b_1 \oplus b_3 \oplus 1, \quad b^4 = b_1 \oplus b_2 \oplus b_3 \oplus 1, \quad (26)$$

and set

$$\begin{aligned} |\Psi_{000}\rangle &= |\Psi_0^0\rangle, \quad |\Psi_{001}\rangle = |\Psi_0^1\rangle, \quad |\Psi_{010}\rangle = |\Psi_1^0\rangle, \quad |\Psi_{011}\rangle = |\Psi_1^1\rangle, \\ |\Psi_{100}\rangle &= |\Psi_2^0\rangle, \quad |\Psi_{101}\rangle = |\Psi_2^1\rangle, \quad |\Psi_{110}\rangle = |\Psi_3^0\rangle, \quad |\Psi_{111}\rangle = |\Psi_3^1\rangle. \end{aligned} \quad (27)$$

In fact, such a joint measurement allows Bob to perform entanglement swapping to three distant Alices. To see this, we can rewrite the combined system including six qubits in the EJM basis, as

$$|\Psi^+\rangle_{A_1 B_1} |\Psi^+\rangle_{A_2 B_2} |\Psi^+\rangle_{A_3 B_3} = \frac{1}{2\sqrt{2}} \sum_{b_1 b_2 b_3} |\tilde{\Psi}_{b_1 b_2 b_3}\rangle_{A_1 A_2 A_3} |\Psi_{b_1 b_2 b_3}\rangle_{B_1 B_2 B_3}, \quad (28)$$

where  $|\tilde{\Psi}_{b_1 b_2 b_3}\rangle = \sigma_x \sigma_x \sigma_x |\Psi_{b_1 b_2 b_3}\rangle^*$ , whose components are complex conjugates of the corresponding components of the state  $|\Psi_{b_1 b_2 b_3}\rangle$ , followed by applying a set of NOT gates, one for each of the three qubits.

In this situation, the correlator reads

$$\langle A_{x_1}^1 A_{x_2}^2 A_{x_3}^3 B^m \rangle = \frac{1}{2^3} \text{tr} \left[ \sum_{b_1 b_2 b_3, b'_1 b'_2 b'_3} (|\tilde{\Psi}_{b_1 b_2 b_3}\rangle \langle \tilde{\Psi}_{b'_1 b'_2 b'_3}| \otimes |\Psi_{b_1 b_2 b_3}\rangle \langle \Psi_{b'_1 b'_2 b'_3}|) (A_{x_1}^1 \otimes A_{x_2}^2 \otimes A_{x_3}^3 \otimes B^m) \right]. \quad (29)$$

Noting that  $A_0^i + A_1^i = \sqrt{2}\sigma_x$  and  $A_0^i - A_1^i = \sqrt{2}\sigma_z$ , then we have

$$I_m = \frac{1}{16\sqrt{2}} \text{tr} \left[ \sum_{b_1 b_2 b_3, b'_1 b'_2 b'_3} (|\tilde{\Psi}_{b_1 b_2 b_3}\rangle \langle \tilde{\Psi}_{b'_1 b'_2 b'_3}| \otimes |\Psi_{b_1 b_2 b_3}\rangle \langle \Psi_{b'_1 b'_2 b'_3}|) (A^m \otimes B^m) \right], \quad (30)$$

where  $A^1 = \sigma_x \sigma_x \sigma_x$ ,  $A^2 = \sigma_z \sigma_z \sigma_x$ ,  $A^3 = \sigma_z \sigma_x \sigma_z$ , and  $A^4 = \sigma_x \sigma_z \sigma_z$ . Substituting Eqs. (24) and (25) into this expression yields

$$I_m = \frac{1}{16\sqrt{2}} \left( \sum_{b_1 b_2 b_3} \delta_{0, b^m} \langle \tilde{\Psi}_{b_1 b_2 b_3} | A^m | \tilde{\Psi}_{b_1 b_2 b_3} \rangle - \sum_{b_1 b_2 b_3} \delta_{1, b^m} \langle \tilde{\Psi}_{b_1 b_2 b_3} | A^m | \tilde{\Psi}_{b_1 b_2 b_3} \rangle \right). \quad (31)$$

Now, according to Eqs. (26) and (27), we calculate the inner products  $\langle \tilde{\Psi}_{b_1 b_2 b_3} | A^m | \tilde{\Psi}_{b_1 b_2 b_3} \rangle$ . A detailed calculation can be found in the appendix C. Substituting the results into (31) leads to

$$I_1 = \frac{1}{8} z \sin(2\gamma) \cos[2(\varphi - \varphi_z)] \sin(\varphi + \frac{\pi}{4}), \quad (32)$$

$$I_2 = \frac{1}{4} z \sin(2\gamma) \sin(\varphi + \frac{\pi}{4}), \quad (33)$$

$$I_3 = \frac{1}{4\sqrt{2}} z (1 + \sin\theta) \cos(\varphi - \varphi_z + \frac{\pi}{4}), \quad (34)$$

and

$$I_4 = \frac{1}{4\sqrt{2}} z(1 + \sin \theta) \sin(\varphi - \varphi_z + \frac{\pi}{4}). \quad (35)$$

Based on these trilocal correlation quantities, we thus have

$$\begin{aligned} \sum_{m=1}^4 |I_m|^{1/3} &= \frac{\sqrt[3]{|z|}}{2} [|\sin(2\gamma) \cos[2(\varphi - \varphi_z)] \sin(\varphi + \frac{\pi}{4})|^{\frac{1}{3}} + |2 \sin(2\gamma) \sin(\varphi + \frac{\pi}{4})|^{\frac{1}{3}} \\ &+ |\sqrt{2}(1 + \sin \theta) \cos(\varphi - \varphi_z + \frac{\pi}{4})|^{\frac{1}{3}} + |\sqrt{2}(1 + \sin \theta) \sin(\varphi - \varphi_z + \frac{\pi}{4})|^{\frac{1}{3}}]. \end{aligned} \quad (36)$$

Using numerical analysis we obtain the maximum value of the quantum prediction 2.2968 with  $\gamma = \pi/4$ ,  $\theta = \pi/2$ ,  $z = 1$  (thus  $\varphi_z = \pi/2$ ) and  $\varphi = 0.1781$  rad (or 1.3921 rad). Taking  $\gamma = \pi/4$  and  $\theta = \pi/2$ , i.e.,  $\tau = 1$ , we provide a plot of the quantum predictions in the range  $\varphi \in [0, \pi]$ , for  $z = 1/\sqrt{3}$ ,  $z = 1/\sqrt{2}$ , and  $z = 1$ , respectively, as shown schematically in Fig.2. It indicates that the quantum predictions vary continuously with  $\varphi$ , and the trilocal inequality (23) can be violated for  $z = 1$  and  $z = 1/\sqrt{2}$ .

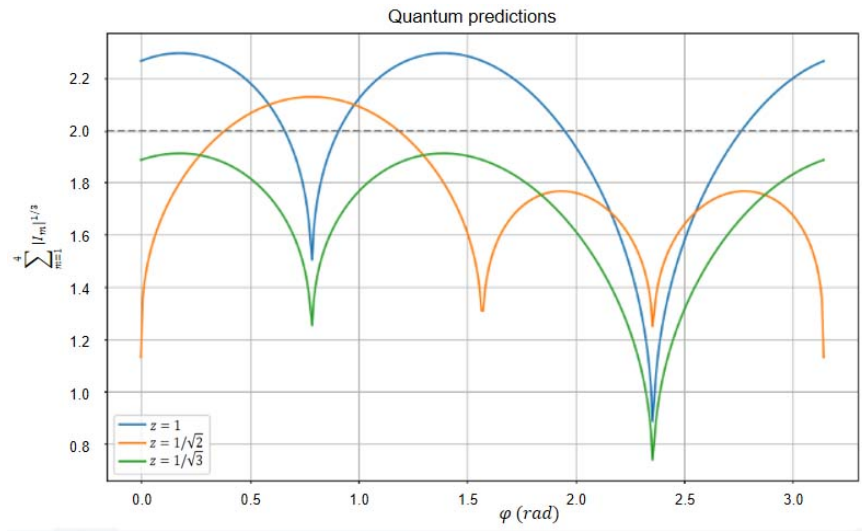


FIG. 2: (color online). A plot of the quantum predictions in the range  $\varphi \in [0, \pi]$ , for  $z = 1$  (blue line),  $z = 1/\sqrt{2}$  (orange line), and  $z = 1/\sqrt{3}$  (green line), respectively.

## V. N-QUBIT SYMMETRIC JOINT MEASUREMENTS

In this section, we provide the generalized  $n$ -qubit symmetric joint measurements for  $n > 3$ . Consider the single-qubit bases  $\{|\pm m_i\rangle\}$ ,  $i = 0, 1, 2, 3$ , two-qubit EJM bases  $\{|\Phi_i\rangle\}_{i=0}^3$  and  $\{|\Phi'_i\rangle\}_{i=0}^3$ , as described earlier. We define the  $n$ -qubit symmetric joint measurements: for  $n$  is even,

$$|\Psi_{i j_1 \dots j_k}\rangle = \cos \gamma |\Phi_i\rangle |\Phi_{j_1}\rangle \dots |\Phi_{j_k}\rangle + (-1)^{[\frac{k}{2}]} \sin \gamma |\Phi'_i\rangle |\Phi'_{j_1}\rangle \dots |\Phi'_{j_k}\rangle, \quad (37)$$

where  $i, j_1, \dots, j_k = 0, 1, 2, 3$ ,  $k = n/2 - 1$ ; for  $n$  is odd,

$$|\Psi_{i j_1 \dots j_k}^0\rangle = \cos \gamma |\Phi_i\rangle |\Phi_{j_1}\rangle \dots |\Phi_{j_k}\rangle |m_i\rangle + (-1)^{[\frac{k}{2}]} \sin \gamma |\Phi'_i\rangle |\Phi'_{j_1}\rangle \dots |\Phi'_{j_k}\rangle | - m_i\rangle \quad (38)$$

and

$$|\Psi_{i j_1 \dots j_k}^1\rangle = \cos \gamma |\Phi_i\rangle |\Phi_{j_1}\rangle \dots |\Phi_{j_k}\rangle | - m_i\rangle - (-1)^{[\frac{k}{2}]} \sin \gamma |\Phi'_i\rangle |\Phi'_{j_1}\rangle \dots |\Phi'_{j_k}\rangle |m_i\rangle, \quad (39)$$

where  $i, j_1, \dots, j_k = 0, 1, 2, 3$ ,  $k = (n - 1)/2 - 1$ .

Note that there are two fundamental components that form the  $n$ -qubit symmetric joint measurements. For an even  $n$ , it is depicted with paired two-qubit EJM bases; for an odd  $n$ , four sets of additional single-qubit base  $\{|\pm m_i\rangle\}$ ,  $i = 0, 1, 2, 3$ , are added. So, a calculation similar to three-qubit EJM basis yields the orthogonality relations

$$\langle \Psi_{ij_1 \dots j_k} | \Psi_{i'j'_1 \dots j'_k} \rangle = \delta_{ii'} \delta_{j_1 j'_1} \dots \delta_{j_k j'_k}, \quad i, i', j_1, j'_1, \dots, j_k, j'_k = 0, 1, 2, 3, \quad (40)$$

for  $n$  is even, and

$$\langle \Psi_{ij_1 \dots j_k}^l | \Psi_{i'j'_1 \dots j'_k}^{l'} \rangle = \delta_{ii'} \delta_{j_1 j'_1} \dots \delta_{j_k j'_k} \delta_{ll'}, \quad i, i', j_1, j'_1, \dots, j_k, j'_k = 0, 1, 2, 3, \quad l, l' = 0, 1, \quad (41)$$

for  $n$  is odd. Using  $\sum_{j_k=0}^3 |\Phi_{j_k}\rangle \langle \Phi_{j_k}| = \sum_{j_k=0}^3 |\Phi'_{j_k}\rangle \langle \Phi'_{j_k}|$ , in the same way, we have the completeness relations

$$\sum_{i, j_1, \dots, j_k=0}^3 |\Psi_{ij_1 \dots j_k}\rangle \langle \Psi_{ij_1 \dots j_k}| = I, \quad (42)$$

for  $n$  is even, and

$$\sum_{i, j_1, \dots, j_k=0}^3 (|\Psi_{ij_1 \dots j_k}^0\rangle \langle \Psi_{ij_1 \dots j_k}^0| + |\Psi_{ij_1 \dots j_k}^1\rangle \langle \Psi_{ij_1 \dots j_k}^1|) = I, \quad (43)$$

for  $n$  is odd.

For an odd-qubit EJM basis, there is one qubit whose reduced states correspond to  $\pm \cos(2\gamma)\vec{m}_i$ , while all the remaining single-qubit reduced states correspond to  $[(1/2)\sqrt{1+2\cos^2(2\gamma)}\cos\theta]\vec{m}'_i$  or  $-[(1/2)\sqrt{1+2\cos^2(2\gamma)}\cos\theta]\vec{m}'_i$ . All single-qubit reductions of even-qubit basis states match the points  $[(1/2)\sqrt{1+2\cos^2(2\gamma)}\cos\theta]\vec{m}'_i$  or  $-[(1/2)\sqrt{1+2\cos^2(2\gamma)}\cos\theta]\vec{m}'_i$ . As described earlier in the three-qubit EJM basis, these reductions can form vertices of pairs of mirror-image tetrahedra within the Bloch sphere, and thus the equations

$$\sum_P P \left[ \sum_{i, j_1, \dots, j_k, l} \langle \Psi_{ij_1 \dots j_k}^l | \vec{\sigma} \otimes I^{\otimes(n-1)} | \Psi_{ij_1 \dots j_k}^l \rangle \right] = 0 \quad (44)$$

hold for all odd-qubit EJM bases, and

$$\sum_P P \left[ \sum_{i, j_1, \dots, j_k} \langle \Psi_{ij_1 \dots j_k} | \vec{\sigma} \otimes I^{\otimes(n-1)} | \Psi_{ij_1 \dots j_k} \rangle \right] = 0 \quad (45)$$

hold for all even-qubit EJM bases, where  $P$  runs over all permutations of the position of “ $\vec{\sigma}$ .” Moreover, in fact, the vertices of these mirror-image tetrahedra can always form a rectangular parallelepiped. Based on this, it can also be interpreted as rectangular-parallelepiped (or hexahedral) symmetry. For the sake of clarity, we are providing a diagram here to illustrate the hexahedral symmetry for the current  $n$ -qubit EJM, as shown in Fig.3.

## VI. CONCLUSION

In summary, we studied a generalization of the two-qubit EJM [4, 5, 15] to one involving  $n$  qubits. To do this, we first defined a three-qubit symmetric joint measurement basis by using the three-parameter two-qubit EJM basis and four sets of single-qubit bases. Since these basis states correspond to the vertices of a tetrahedron located on the Bloch sphere [15], the current architecture ensures that it has the tetrahedral (or hexahedral) symmetry for the single-qubit reductions. In addition to symmetry, we also demonstrated its application to a trilocal star-shaped network. More importantly, as a general method, it can be naturally extended to  $n$ -qubit EJM, preserving the elegant symmetry.

In applying it to the star-network nonlocality, however, we found that the example provided does not currently result in the maximum violation [7]. Note that, in the given measurement settings, the quantum prediction, in general, varies with the parameters  $\gamma$ ,  $\theta$ ,  $z$ , and  $\varphi$ . By numerically optimizing the measurement settings, it may be possible to further enhance the quantum prediction value, potentially bringing it to or near its maximum value of  $2\sqrt{2}$ . Nevertheless, it is indeed an interesting issue of principle to develop the symmetric quantum joint measurements on multiple qubits, which could potentially lead to new insights into the fundamental nature of quantum measurement and advance the field of quantum information processing.

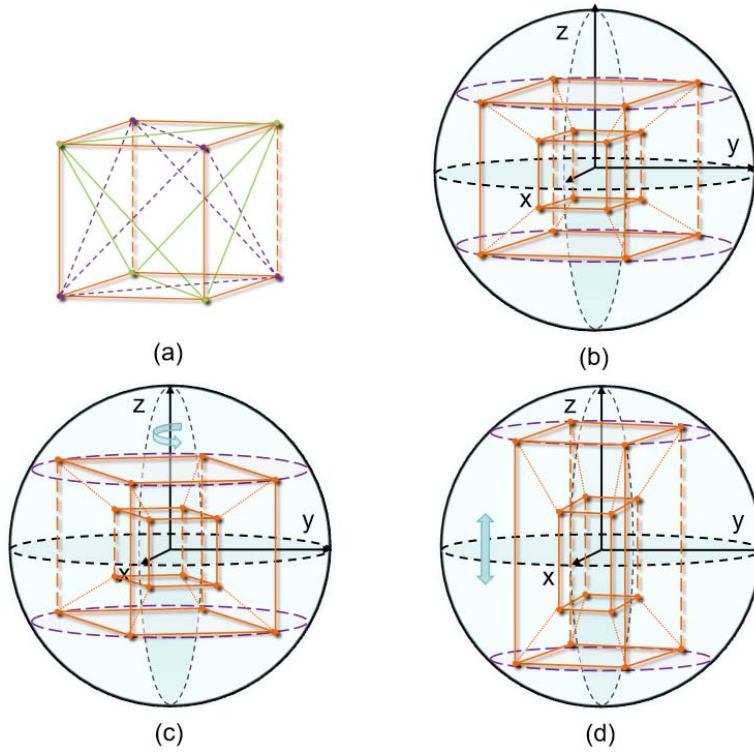


FIG. 3: The schematic diagram illustrating hexahedral symmetry of the generalized multi-qubit EJM: (a) The correspondence relationship between the vertices of a hexahedron and two tetrahedra; (b) the reduced states and the corresponding unit vectors to which they point; (c) the set of reduced states associated with an arbitrary rotation around the  $z$ -axis; and (d) the set of reduced states associated with a stretch along the  $z$ -axis.

### Acknowledgments

This work was supported by the Hebei Science and Technology Program Foundation of China under Grant No. 246Z0902G, the National Natural Science Foundation of China under Grant No. 62271189, and the Hebei High-level Talents Foundation of China under Grant No: A202101002.

### Appendix A: Proof of the orthogonality and completeness for the three-qubit EJM

We first see the orthogonality of the three-qubit EJM basis states. Note that each single-qubit basis state  $|m_i\rangle$  is orthogonal to  $| -m_i\rangle$  and two-qubit basis states satisfy  $\langle\Phi_i|\Phi_j\rangle = \delta_{ij}$ ,  $i, j = 0, 1, 2, 3$ . Also, for  $i = 0, 1$ ,  $|\Phi'_i\rangle = |\Phi_{i+2}\rangle$ , and for  $i = 2, 3$ ,  $|\Phi'_i\rangle = |\Phi_{i-2}\rangle$ . Thus, for  $i = j$ , we can directly see that

$$\langle\Psi_i^k|\Psi_i^l\rangle = \cos^2\gamma\langle\Phi_i|\Phi_i\rangle\delta_{kl} + \sin^2\gamma\langle\Phi'_i|\Phi'_i\rangle\delta_{kl} = \delta_{kl}, \quad i = 0, 1, 2, 3, k, l = 0, 1. \quad (\text{A1})$$

For  $i \neq j$ , it is divided into three cases: (i)  $i = 0, 2$ , and  $j = 1, 3$ , or vice versa; (ii)  $i, j = 0, 2$ ; and (iii)  $i, j = 1, 3$ . For  $i = 0, 2$  and  $j = 1, 3$  (or vice versa), using  $\langle\Phi_i|\Phi_j\rangle = 0$ , we can easily verify that  $\langle\Psi_i^k|\Psi_j^l\rangle = 0$ . For  $i, j = 0, 2$ , we calculate  $\langle\Psi_0^k|\Psi_2^l\rangle$ ,  $k, l = 0, 1$ , as

$$\langle\Psi_0^0|\Psi_2^1\rangle = -\langle\Psi_0^1|\Psi_2^0\rangle = \sin\gamma\cos\gamma(\langle m_0|m_2\rangle + \langle -m_0|-m_2\rangle), \quad (\text{A2})$$

and

$$\langle\Psi_0^k|\Psi_2^k\rangle = \sin\gamma\cos\gamma(\langle -m_0|m_2\rangle - \langle m_0|-m_2\rangle), \quad k = 0, 1. \quad (\text{A3})$$

Note that  $\langle -m_0|-m_2\rangle = -\langle m_0|m_2\rangle = zi$ ,  $\langle -m_0|m_2\rangle = \langle m_0|-m_2\rangle = -i\sqrt{1-z^2}$ . So we have  $\langle\Psi_0^k|\Psi_2^l\rangle = 0$ , and thus  $\langle\Psi_2^l|\Psi_0^k\rangle = (\langle\Psi_0^k|\Psi_2^l\rangle)^\dagger = 0$ . Similarly, for  $i, j = 1, 3$ , using  $\langle -m_1|-m_3\rangle = -\langle m_1|m_3\rangle = zi$  and  $\langle -m_1|m_3\rangle = \langle m_1|-m_3\rangle = i\sqrt{1-z^2}$ , one can obtain  $\langle\Psi_1^k|\Psi_3^l\rangle = \langle\Psi_3^k|\Psi_1^l\rangle = 0$ ,  $k, l = 0, 1$ .



Thus we have the orthogonality relations

$$\langle \Psi_i^k | \Psi_j^l \rangle = \delta_{ij} \delta_{kl}, \quad i, j = 0, 1, 2, 3, k, l = 0, 1. \quad (\text{A4})$$

Now let us show the completeness relation by calculating the outer product  $\sum_{i,k} |\Psi_i^k\rangle\langle\Psi_i^k|$ ,  $i = 0, 1, 2, 3; k = 0, 1$ . For  $i = 0, 1$ , a straightforward calculation by Eqs. (10) and (11) shows that

$$\begin{aligned} \sum_{k=0,1} |\Psi_i^k\rangle\langle\Psi_i^k| &= (\cos^2 \gamma |\Phi_i\rangle\langle\Phi_i| + \sin^2 \gamma |\Phi_{i+2}\rangle\langle\Phi_{i+2}|) \otimes (|m_i\rangle\langle m_i| + |-m_i\rangle\langle -m_i|) \\ &+ \cos \gamma \sin \gamma [ (|\Phi_i\rangle\langle\Phi_{i+2}| - |\Phi_{i+2}\rangle\langle\Phi_i|) \otimes (|m_i\rangle\langle -m_i| - |-m_i\rangle\langle m_i|) ]. \end{aligned} \quad (\text{A5})$$

Similarly, for  $i = 2, 3$ , we have

$$\begin{aligned} \sum_{k=0,1} |\Psi_i^k\rangle\langle\Psi_i^k| &= (\cos^2 \gamma |\Phi_i\rangle\langle\Phi_i| + \sin^2 \gamma |\Phi_{i-2}\rangle\langle\Phi_{i-2}|) \otimes (|m_i\rangle\langle m_i| + |-m_i\rangle\langle -m_i|) \\ &- \cos \gamma \sin \gamma [ (|\Phi_i\rangle\langle\Phi_{i-2}| - |\Phi_{i-2}\rangle\langle\Phi_i|) \otimes (|m_i\rangle\langle -m_i| - |-m_i\rangle\langle m_i|) ], \end{aligned} \quad (\text{A6})$$

Using completeness relation  $|m_i\rangle\langle m_i| + |-m_i\rangle\langle -m_i| = I$  and summing over the ensemble yields

$$\begin{aligned} \sum_{i=0}^3 \sum_{k=0}^1 |\Psi_i^k\rangle\langle\Psi_i^k| &= \left( \sum_{i=0}^3 |\Phi_i\rangle\langle\Phi_i| \right) \otimes I + \cos \gamma \sin \gamma (|\Phi_0\rangle\langle\Phi_2| - |\Phi_2\rangle\langle\Phi_0|) \otimes \sum_{i=0,2} (|m_i\rangle\langle -m_i| - |-m_i\rangle\langle m_i|) \\ &+ \cos \gamma \sin \gamma (|\Phi_1\rangle\langle\Phi_3| - |\Phi_3\rangle\langle\Phi_1|) \otimes \sum_{i=1,3} (|m_i\rangle\langle -m_i| - |-m_i\rangle\langle m_i|). \end{aligned} \quad (\text{A7})$$

We note that  $|m_i\rangle\langle -m_i| - |-m_i\rangle\langle m_i| = e^{i\varphi_i}|1\rangle\langle 0| - e^{-i\varphi_i}|0\rangle\langle 1|$  and thus  $\sum_{i=0,2} (|m_i\rangle\langle -m_i| - |-m_i\rangle\langle m_i|) = \sum_{i=1,3} (|m_i\rangle\langle -m_i| - |-m_i\rangle\langle m_i|) = 0$ . So, combining these results yields

$$\sum_{i=0}^3 \sum_{k=0}^1 |\Psi_i^k\rangle\langle\Psi_i^k| = \sum_{i=0}^3 |\Phi_i\rangle\langle\Phi_i| \otimes I = I. \quad (\text{A8})$$

## Appendix B: Reductions of the three-qubit EJM basis states

We here calculate the reductions of the three-qubit EJM basis states by tracing out two qubits. Basing directly on the Eqs. (10) and (11) and noting that  $\langle m_i | I | m_i \rangle = \langle -m_i | I | -m_i \rangle = 1$ ,  $\langle m_i | I | -m_i \rangle = \langle -m_i | I | m_i \rangle = 0$ , we have

$$\langle \Psi_i^k | \vec{\sigma} \otimes I \otimes I | \Psi_i^k \rangle = \cos^2 \gamma \langle \Phi_i | \vec{\sigma} \otimes I | \Phi_i \rangle + \sin^2 \gamma \langle \Phi_{i+2} | \vec{\sigma} \otimes I | \Phi_{i+2} \rangle, \quad i = 0, 1, \quad (\text{B1})$$

and

$$\langle \Psi_i^k | \vec{\sigma} \otimes I \otimes I | \Psi_i^k \rangle = \cos^2 \gamma \langle \Phi_i | \vec{\sigma} \otimes I | \Phi_i \rangle + \sin^2 \gamma \langle \Phi_{i-2} | \vec{\sigma} \otimes I | \Phi_{i-2} \rangle, \quad i = 2, 3. \quad (\text{B2})$$

Note that

$$\langle \Phi_i | \vec{\sigma} \otimes I | \Phi_i \rangle = \frac{1}{\sqrt{2}} \cos \theta (\cos(\varphi_i - \varphi_z), \sin(\varphi_i - \varphi_z), (-1)^i / \sqrt{2}), \quad i = 0, 1, 2, 3, \quad (\text{B3})$$

$\cos(\varphi_{i\pm 2} - \varphi_z) = -\cos(\varphi_i - \varphi_z)$  and  $\sin(\varphi_{i\pm 2} - \varphi_z) = -\sin(\varphi_i - \varphi_z)$ . Substituting we obtain

$$\langle \Psi_i^k | \vec{\sigma} \otimes I \otimes I | \Psi_i^k \rangle = \frac{1}{2} \cos \theta (\sqrt{2} \cos(2\gamma) \cos(\varphi_i - \varphi_z), \sqrt{2} \cos(2\gamma) \sin(\varphi_i - \varphi_z), (-1)^i), \quad i = 0, 1, 2, 3. \quad (\text{B4})$$

Let

$$\vec{m}'_i = \frac{1}{\sqrt{1 + 2 \cos^2(2\gamma)}} (\sqrt{2} \cos(2\gamma) \cos(\varphi_i - \varphi_z), \sqrt{2} \cos(2\gamma) \sin(\varphi_i - \varphi_z), (-1)^i), \quad (\text{B5})$$

and then we have

$$\langle \Psi_i^k | \vec{\sigma} \otimes I \otimes I | \Psi_i^k \rangle = \frac{1}{2} [\sqrt{1 + 2 \cos^2(2\gamma)} \cos \theta] \vec{m}'_i. \quad (\text{B6})$$

A similar calculation for  $\langle \Psi_i^k | I \otimes \vec{\sigma} \otimes I | \Psi_i^k \rangle$  yields

$$\langle \Psi_i^k | I \otimes \vec{\sigma} \otimes I | \Psi_i^k \rangle = -\frac{1}{2}[\sqrt{1+2\cos^2(2\gamma)} \cos \theta] \vec{m}'_i. \quad (\text{B7})$$

To proceed, by using  $\langle \Phi_i | \Phi_j \rangle = \delta_{ij}$ , we have

$$\langle \Psi_i^0 | I \otimes I \otimes \vec{\sigma} | \Psi_i^0 \rangle = \cos^2 \gamma \langle m_i | \vec{\sigma} | m_i \rangle + \sin^2 \gamma \langle -m_i | \vec{\sigma} | -m_i \rangle, \quad (\text{B8})$$

and

$$\langle \Psi_i^1 | I \otimes I \otimes \vec{\sigma} | \Psi_i^1 \rangle = \cos^2 \gamma \langle -m_i | \vec{\sigma} | -m_i \rangle + \sin^2 \gamma \langle m_i | \vec{\sigma} | m_i \rangle, \quad (\text{B9})$$

for  $i = 0, 1, 2, 3$ . Then using  $\langle m_i | \vec{\sigma} | m_i \rangle = \vec{m}_i$  and  $\langle -m_i | \vec{\sigma} | -m_i \rangle = -\vec{m}_i$ , we have

$$\langle \Psi_i^k | I \otimes I \otimes \vec{\sigma} | \Psi_i^k \rangle = (-1)^k \cos(2\gamma) \vec{m}_i, \quad (\text{B10})$$

where  $\vec{m}_i = (\sqrt{1-z_i^2} \cos \varphi_i, \sqrt{1-z_i^2} \sin \varphi_i, z_i)$ ,  $i = 0, 1, 2, 3$ .

### Appendix C: Derivation of the trilocal correlation quantities

By using one-to-one correspondences (27), we here rewrite the three-qubit EJM basis as

$$|\Psi_{000}\rangle = \cos \gamma |\Phi_0\rangle |m_0\rangle + \sin \gamma |\Phi_2\rangle | -m_0\rangle, \quad |\Psi_{001}\rangle = \cos \gamma |\Phi_0\rangle | -m_0\rangle - \sin \gamma |\Phi_2\rangle |m_0\rangle, \quad (\text{C1})$$

$$|\Psi_{010}\rangle = \cos \gamma |\Phi_1\rangle |m_1\rangle + \sin \gamma |\Phi_3\rangle | -m_1\rangle, \quad |\Psi_{011}\rangle = \cos \gamma |\Phi_1\rangle | -m_1\rangle - \sin \gamma |\Phi_3\rangle |m_1\rangle, \quad (\text{C2})$$

$$|\Psi_{100}\rangle = \cos \gamma |\Phi_2\rangle |m_2\rangle - \sin \gamma |\Phi_0\rangle | -m_2\rangle, \quad |\Psi_{101}\rangle = \cos \gamma |\Phi_2\rangle | -m_2\rangle + \sin \gamma |\Phi_0\rangle |m_2\rangle, \quad (\text{C3})$$

$$|\Psi_{110}\rangle = \cos \gamma |\Phi_3\rangle |m_3\rangle - \sin \gamma |\Phi_1\rangle | -m_3\rangle, \quad |\Psi_{111}\rangle = \cos \gamma |\Phi_3\rangle | -m_3\rangle + \sin \gamma |\Phi_1\rangle |m_3\rangle. \quad (\text{C4})$$

Next, we take  $\langle \tilde{\Psi}_{000} | A^1 | \tilde{\Psi}_{000} \rangle$  as an example to give a detailed derivation to calculate the trilocal correlation quantities.

We calculate  $|\tilde{\Psi}_{000}\rangle$  and have

$$\begin{aligned} |\tilde{\Psi}_{000}\rangle = & \frac{1 + i\sqrt{3z^2 - 1}}{2\sqrt{3z^2}} [-d_1^+ e^{-i(\frac{3}{2}\varphi - \varphi_z)} |000\rangle - d_0^- e^{-i(\frac{1}{2}\varphi - \varphi_z)} |001\rangle - d_1^- (r_-^\theta)^* e^{-i\frac{\varphi}{2}} |010\rangle - d_0^+ (r_-^\theta)^* e^{i\frac{\varphi}{2}} |011\rangle \\ & - d_1^- (r_+^\theta)^* e^{-i\frac{\varphi}{2}} |100\rangle - d_0^+ (r_+^\theta)^* e^{i\frac{\varphi}{2}} |101\rangle + d_1^+ e^{i(\frac{1}{2}\varphi - \varphi_z)} |110\rangle + d_0^- e^{i(\frac{3}{2}\varphi - \varphi_z)} |111\rangle], \end{aligned} \quad (\text{C5})$$

where  $d_0^\pm = (\cos \gamma \sqrt{1+z} \pm \sin \gamma \sqrt{1-z})/\sqrt{2}$ ,  $d_1^\pm = (\cos \gamma \sqrt{1-z} \pm \sin \gamma \sqrt{1+z})/\sqrt{2}$ , and  $(r_\pm^\theta)^* = (1 \pm e^{-i\theta})/\sqrt{2}$ . Substituting  $A^1 = \sigma_x \sigma_x \sigma_x$  yields

$$\langle \tilde{\Psi}_{000} | \sigma_x \sigma_x \sigma_x | \tilde{\Psi}_{000} \rangle = -\frac{1}{2}[\sqrt{1-z^2} \cos(2\gamma) + z \sin(2\gamma)] \cos[2(\varphi - \varphi_z)] \cos \varphi. \quad (\text{C6})$$

Similarly, we calculate all of the inner products  $\langle \tilde{\Psi}_{b_1 b_2 b_3} | \sigma_x \sigma_x \sigma_x | \tilde{\Psi}_{b_1 b_2 b_3} \rangle$ . Also, considering definition of bits  $b_1, b_2, b_3$  (26) we have

$$M_0^1 = |\Psi_{001}\rangle \langle \Psi_{001}| + |\Psi_{010}\rangle \langle \Psi_{010}| + |\Psi_{101}\rangle \langle \Psi_{101}| + |\Psi_{110}\rangle \langle \Psi_{110}| \quad (\text{C7})$$

and

$$M_1^1 = |\Psi_{000}\rangle \langle \Psi_{000}| + |\Psi_{011}\rangle \langle \Psi_{011}| + |\Psi_{100}\rangle \langle \Psi_{100}| + |\Psi_{111}\rangle \langle \Psi_{111}|. \quad (\text{C8})$$

So, substituting these into (31) we have

$$I_1 = \frac{1}{8} z \sin(2\gamma) \cos[2(\varphi - \varphi_z)] \sin(\varphi + \frac{\pi}{4}). \quad (\text{C9})$$

A calculation similar to  $I_1$  yields

$$I_2 = \frac{1}{4}z \sin(2\gamma) \sin(\varphi + \frac{\pi}{4}), \quad (\text{C10})$$

$$I_3 = \frac{1}{4\sqrt{2}}z(1 + \sin\theta) \cos(\varphi - \varphi_z + \frac{\pi}{4}), \quad (\text{C11})$$

and

$$I_4 = \frac{1}{4\sqrt{2}}z(1 + \sin\theta) \sin(\varphi - \varphi_z + \frac{\pi}{4}). \quad (\text{C12})$$

- 
- [1] M. A. Nielsen and I. L. Chuang, *Quantum Computation and Quantum Information* (Cambridge University Press, Cambridge, 2000).
- [2] R. Horodecki, P. Horodecki, M. Horodecki, and K. Horodecki, Quantum entanglement, *Rev. Mod. Phys.* **81**, 865–942 (2009).
- [3] O. Gühne and G. Tóth, Entanglement detection, *Phys. Rep.* **474**, 1–75 (2009).
- [4] N. Gisin, Entanglement 25 years after quantum teleportation: testing joint measurements in quantum networks, *Entropy* **21**, 325 (2019).
- [5] A. Tavakoli, N. Gisin, and C. Branciard, Bilocal Bell inequalities violated by the quantum elegant joint measurement, *Phys. Rev. Lett.* **126**, 220401 (2021).
- [6] C. Branciard, N. Gisin, and S. Pironio, Characterizing the nonlocal correlations created via entanglement swapping, *Phys. Rev. Lett.* **104**, 170401 (2010).
- [7] A. Tavakoli, P. Skrzypczyk, D. Cavalcanti, and A. Acín, Nonlocal correlations in the star-network configuration, *Phys. Rev. A* **90**, 062109 (2014).
- [8] M. X. Luo, Computationally efficient nonlinear Bell inequalities for quantum networks, *Phys. Rev. Lett.* **120**, 140402 (2018).
- [9] A. Pozas-Kerstjens, R. Rabelo, L. Rudnicki, R. Chaves, D. Cavalcanti, M. Navascués, and A. Acín, Bounding the sets of classical and quantum correlations in networks, *Phys. Rev. Lett.* **123**, 140503 (2019).
- [10] A. Pozas-Kerstjens, N. Gisin, and A. Tavakoli, Full network nonlocality, *Phys. Rev. Lett.* **128**, 010403 (2022).
- [11] A. Tavakoli, A. Pozas-Kerstjens, M. X. Luo, and M. O. Renou, Bell nonlocality in networks, *Rep. Prog. Phys.* **85**, 056001 (2022).
- [12] E. Bäumer, N. Gisin, and A. Tavakoli, Demonstrating the power of quantum computers, certification of highly entangled measurements and scalable quantum nonlocality, *NPJ Quantum Inform.* **7**, 117 (2021).
- [13] C. X. Huang, X. M. Hu, Y. Guo, C. Zhang, B. H. Liu, Y. F. Huang, C. F. Li, G. C. Guo, N. Gisin, C. Branciard, and A. Tavakoli, Entanglement swapping and quantum correlations via symmetric joint measurements, *Phys. Rev. Lett.* **129**, 030502 (2022).
- [14] F. Del Santo, J. Czartowski, K. Zyczkowski, and N. Gisin, Iso-entangled bases and joint measurement, *Phys. Rev. Research* **6**, 023085 (2024).
- [15] Y. Q. He, D. Ding, T. Gao, Z. J. Li, and F. L. Yan, Three-parameter symmetric quantum joint measurement on two qubits, *Phys. Rev. A* **111**, 012429 (2025).
- [16] V. Coffman, J. Kundu, and W. K. Wootters, Distributed entanglement, *Phys. Rev. A* **61**, 052306 (2000).
- [17] F. Pimpel, M. J. Renner, and A. Tavakoli, Do entangled states correspond to entangled measurements under local transformations? *Phys. Rev. A* **108**, 022220 (2023).